

See discussions, stats, and author profiles for this publication at: <https://www.researchgate.net/publication/268436071>

# Finite element simulation of deep rolling and evaluate the influence of parameters on residual stress

Article · January 2012

CITATIONS

4

READS

308

2 authors:



[Afshin Manouchehrifar](#)  
Islamic Azad University

4 PUBLICATIONS 4 CITATIONS

SEE PROFILE



[Kianosh Alasvand](#)

1 PUBLICATION 4 CITATIONS

SEE PROFILE

# Finite element simulation of deep rolling and evaluate the influence of parameters on residual stress

AFSHIN MANOUCHEHRIFAR, KIANOUSH ALASVAND

Dept. of mechanical engineering

Islamic AZAD University – Khomeinishar Branch

Khomeinishar, Iran

Manouchehri@iaukhsh.ac.ir, kianoshaz@gmail.com

**Abstract:** - In general, residual stresses in a body can be harmful or useful. Tensile residual stresses are usually harmful which make the surface of the body brittle and decrease the mechanical strength. Whereas compressive residual stresses are usually useful. There are various techniques to improve resistance of parts in fatigue or oscillating loads. One of the most efficient techniques is inducing residual stress layer in the surface of components. Mechanical surface treatments such as deep rolling, shot peening, and laser peening can significantly improve the fatigue behavior of metallic components with high stress. Deep rolling, also can improve surface quality, dimensional accuracy and mechanical properties of the parts. Compressive residual stress generated by the process reduces the tensile stresses during loading into the workpiece. By this process surface finish can be improved in a very high level as well. These two factors, reducing the tensile stress in part through the creation of compressive residual stress and surface finish, Enhance the fatigue life of the piece. The distribution of residual stress induced by deep rolling can be influenced by rolling parameters such as overlap of the rolling tracks, friction coefficient between roller and target plate, deep rolling with constant force, and deep rolling with mechanical tools. In this work the effect of these parameters are studied by finite element simulations. The material used in this work is Ti-6Al-4V.

**Key-Words:** Residual stress, Finite element, Deep rolling, Titanium alloy, Ti-6Al-4V, elastic-plastic deformation

## 1 Introduction

It is well known that mechanical surface treatments, such as deep rolling, shot peening and laser shock peening, can significantly improve the fatigue behavior of highly-stressed metallic components. Deep rolling (DR) is particularly attractive since it is possible to generate, near the surface, deep compressive residual stresses and work hardened layers while retaining a relatively smooth surface finish. Previous research has shown that the best method to increase the damage tolerance is mechanical strain hardening of the surface layer. This can be achieved by deep rolling. Deep rolling belongs to a group of manufacturing technologies, which are used for the mechanical strain hardening of the surface layer. With regards to the component requirements, deep rolling distinguishes itself by three substantial advantages from all the other mechanical strain hardening methods. The first advantage is that the highest and the deepest compressive residual state of stress can be induced to the component surface layer. The second advantage is a high strain hardening, especially deep

inside the surface layer. The third major advantage of deep rolling is the improvement of the surface quality, especially in comparison to the shot-peening process. Also, in other examinations, a lifetime increase in comparison to shot-peened components could be observed. The results show that significant lifetime increase and decreased crack propagation can be achieved by the deep rolling process in both cases.

In the present work the application of the Finite Element Analysis (FEM) was proposed in order to determine model responses for different process parameters as an effective and cost reducing alternative to an experimental set-up. The FEM enables the prediction of the material behaviour for the specified loading conditions. Thus, the behaviour of Ti-6Al-4V was modelled in ABAQUS. Experimental results in [2], [3] show that the influence of deep rolling reaches up to 500  $\mu\text{m}$ . At the same time, the residual stress gradient in this depth is very high. In order to resolve such high gradients at sufficient accuracy, it is necessary to provide a very fine mesh in the surface layer (Fig.1).

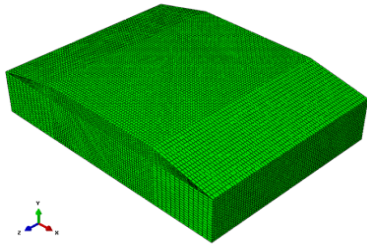


Fig.1: Model mesh requirements

## 2 Literature review

The resistance of the material against fatigue can be increased by surface treatment techniques such as cold deep rolling (CDR) [4], water peening[5], shot peening[6], low plasticity burnishing (LPB) [7], laser shock peening (LSP) [8], ultrasonic shot peening (USP) [9], ultrasonic impact treatment [10]. Fatigue cracking usually originates from the surface of parts undergoing cyclic loading. Surface roughness, residual stress, and near surface microstructure are believed to be the driving factors that control fatigue crack initiation and propagation and hence control the fatigue life of parts [11]. One of the most well known benefits of deep rolling as compared to other surface treatments is the great depth of the affected layer exhibiting alterations of the work hardening state (usually work hardening) and compressive residual stresses [4].

Another one is the generation of glossy surfaces with low roughness as compared to treatments like shot peening. These three effects can significantly enhance the mechanical behaviour of metallic materials, especially under cyclic fatigue loading.

Deep rolling is a surface treatment technique which is performed using roller type instruments to produce a surface compressive residual stress to improve the fatigue resistance of materials and engineering components [4]. The deep rolling technique is widely used in automobile industry, in turbo aircraft engine and turbine blades [4].

The effects of deep rolling on fatigue behaviour have been thoroughly investigated and the influence of notches and material hardness on fatigue strength enhancement of deep rolled components became clear [4]. Even deep rolling was already used in combination with thermal surface treatments such as induction hardening, especially in the automotive industry [4].

Altenberger et. al. [12] investigate the thermal stability of near-surface microstructures induced by deep rolling and laser-shock peening in AISI 304 stainless steels (AISI 304) and Ti-6Al-4V using in-situ transmission electron microscopy. The improvements in fatigue resistance at elevated temperature are related to the high-temperature

stability of the work-hardened nearsurface microstructure. They found The beneficial effect of DR and LSP on the fatigue life at temperatures as high as 550–600°C, where almost complete relaxation of residual stresses has occurred, appears to be related to the thermal stability of the work-hardened near-surface microstructures.

Tolga et. al. [13] shows that UDCR is a reliable and effective surface enhancement technique as it can be used for enhancing the service properties and surface characteristics of Ti-6Al-4V components. In UDCR, the plastic deformation on the part surface can easily be achieved by applying considerably lower pressures as compared to other conventional techniques. High plastic deformation results in deep and high compressive residual stresses in the nearsurface area of treated components. Moreover, work hardening on the surface is achieved. These physical effects lead to improvement of fatigue strength of components as well as increase in resistance to corrosion and foreign objects.

Juijerm et. al. [14] investigated the effect of high-temperature deep rolling on cyclic deformation behavior and shows that deep rolling at elevated temperatures up to approximately 200°C resulted in an increase of near-surface hardnesses of the solution-heat-treated AA6110 compared to conventional deep rolling due to static/dynamic precipitation, whereas lower macroscopic compressive residual stresses and work-hardening states were observed because static/dynamic recovery occurred.

Tsuji et. al. [15] examined surface-modified Ti-6Al-4V alloy by the combination of plasma-carburizing and deep-rolling and shows that deep-rolling effectively improves the surface roughness and induces the highly compressive residual stress and work hardening on the plasma-carburized Ti-6Al-4V surface and near the surface region. Consequently, the fatigue life of plasma-carburized Ti-6Al-4V has been significantly improved by these multiplier effects. The initiation of fatigue fractures of both deep-rolled and deep-rolled carburized samples occurred on the surface at maximum stress levels higher than approximately 900MPa.

Backer et. al. [16] analysed of the deep rolling process on turbine blades using the FEM/BEM-Coupling. And enables the computing of large-scale models at low computational cost and high result accuracy and investigated the effect of the deep rolling on suffer damages caused by the unavoidable impact of foreign objects.

### 3 Finite element modeling

The finite element package ABAQUS 6.10 is used to simulate the procedure corresponding to the experimental operation. Because of it is capable; the explicit dynamic algorithm is used to simulate the numerous impacts. Then a General static algorithm is combined to provide the resulting deformed shape as a spring-back analysis. Deep rolling is performed using a roller and by reciprocating motion. The schematic model of deep rolling is illustrated in Fig. 5(b).

The geometry of material target is assumed as deformable plate with 6mm width, 8mm length and 2 mm height dimensions. The boundary condition is fixed by encastre constraint. The meshes consist of 165888 Eight-node linear brick elements with reduced integration and hourglass control (C3D8R). Simplicity roller is assumed to be a fully spherical discrete rigid with a mass positioned at its centre. Roller is meshed by using sweep technique and quad-dominated element shape. Several of preliminary runs were conducted to establish the appropriate mesh design for Convergence test model. Each shown result consists of two runs model. First run contains an explicit dynamic step by using initial mesh and configuration. Another run contains a static general step by using import part and update reference configuration from output of first run for considering spring back effect.

The material used in this investigation is Ti-6Al-4V. The chemical compositions of the Ti-6Al-4V materials are listed in Table 1.

The material properties are given in Table 2. Also, the material model used in this work is Johnson-Cook model which is described by the relation 1:

$$\sigma = (A + B\varepsilon^n)(1 + C \ln \dot{\varepsilon}^*) (1 - T^{*m}) \quad (1)$$

Where  $\varepsilon$  is the equivalent plastic strain,  $\dot{\varepsilon}^* = \frac{\dot{\varepsilon}}{\dot{\varepsilon}_0}$  is the dimensionless plastic strain rate and  $T^*$  is:

$$T^* = \frac{T - T_{room}}{T_{melt} - T_{room}} \quad (2)$$

$A$ ,  $B$ ,  $C$ ,  $n$  and  $m$  are the material constants where  $A$  is the yield strength,  $B$  and  $n$  are the strain hardening coefficient and exponent,  $C$  is the strain rate coefficient and  $m$  is the thermal softening exponent. The material constants used in the Johnson-Cook equation are presented in Table 3.

Table 1: Chemical composition of the Ti-6Al-4V material

Elements (Wt.%)	Al	C	Fe	H
	5.8	0.03	0.21	0.004
Elements (Wt.%)	N	O	V	Ti
	0.01	0.17	4.08	Bal.

Table 2: Material Properties Used for Simulating Ti-6Al-4V

Density (kg/m <sup>3</sup> )	Elastic Modulus (Gpa)	Poissons Ratio	Thermal Expansion (10 <sup>-6</sup> )/°C	Specific Heat (j/kgK)	Inelastic Heat Fraction
4428	110	0.31	9	580	0.9

Table 3: Johnson-Cook Material Parameters for Ti-6Al-4V

	A (Mpa)	B (Mpa)	n	C	m	T <sub>melt</sub> (°C)
Ti-6Al-4V	862	331	0.34	0.012	0.8	1605

### 4 Model validation

In order to verify the accuracy of the finite element simulation of deep rolling, the residual stress profile was compared with the experimentally obtained data from the literature [1] and is shown in Fig. 2.

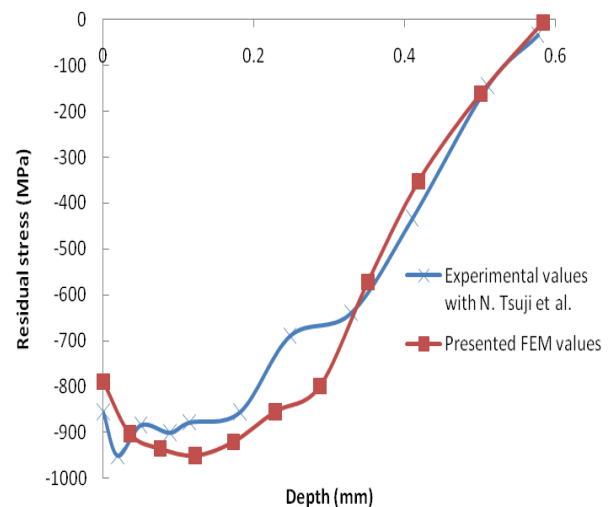


Fig.2: Modeling validation by comparison of residual stress profiles obtained with result experimentally by [1]

As the figure indicates, there is satisfactory agreement between the experimental and numerical results, which provides some verification of the finite element model. The difference between the two graphs can be seen due to lack of information in the experimental test conditions. Modeling conditions are given in Table 4 and Fig.3.

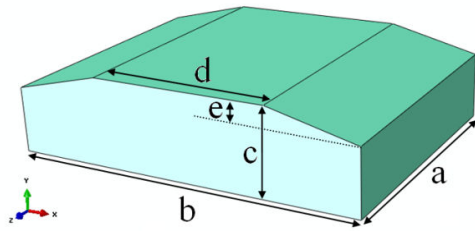


Fig. 3: The model of deep rolling

Table 4: The dimensions of the roller and work piece shown in Fig. 3

Roller		Workpiece	
r	0.9 mm	a	6 mm
h	0.1 mm	b	8 mm
V	10 m/s	c	2 mm
		d	4 mm
		e	0.5 mm

## 5 Numerical results

Five aspects of the deep rolling model are examined in current work. The first is concerned with the effect of overlap, the second is effect of friction coefficient between the roller and target plate, the third is deep rolling with constant force, the fourth is deep rolling with mechanical tools, and the fifth is deep rolling with vibration of workpiece.

All results obtained from variation of residual stress along the path that is created by selecting nodes along the central axis in target plate. The Path is shown in Fig. 4.

The stress distributions in x, y and z directions, indicated in Fig (5), are typically shown in Fig 6. As the figure indicates, the stress component in Y-direction ( $\sigma_{yy}$ ) is not so significant and can be considered negligible. However, the stress component in x-direction ( $\sigma_{xx}$ ), which coincides with rolling direction is considerable but still is significantly lower than the stress component in Z-direction ( $\sigma_{zz}$ ), which is perpendicular to the direction of rolling. However, only the stress component  $\sigma_{xx}$  is considered for evaluation of the effects of the rolling parameters on residual stress distribution, induced by deep rolling in this work.

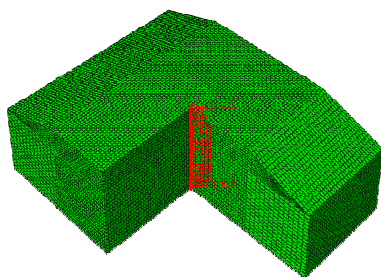


Fig. 4: Path along Y-direction in target plate.

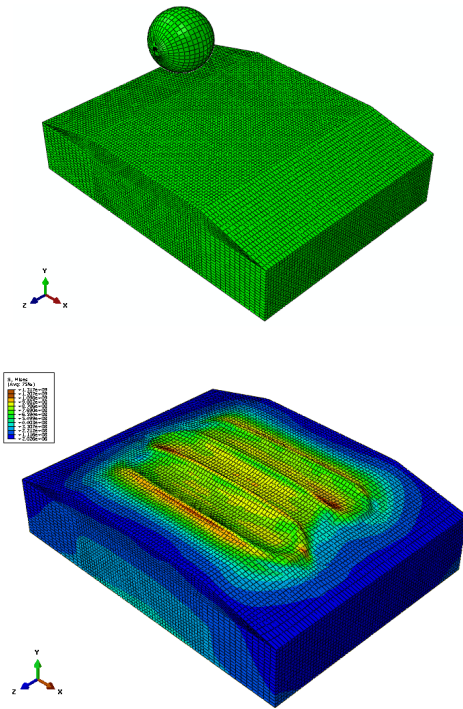


Fig.5 (a) Finite element model of the work piece (b) a deep rolling model

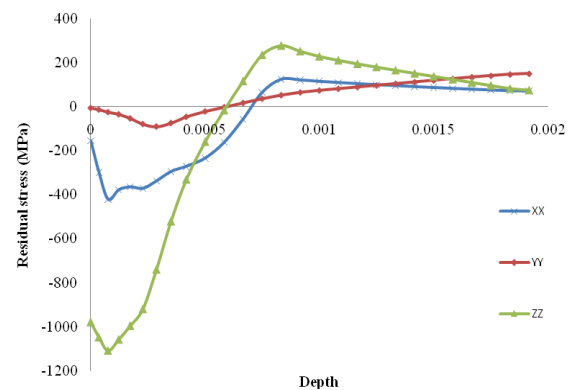


Fig.6. The stress distribution in x, y and z directions

### 5.1 Effect of overlap

The deep rolling finite element analysis is performed to investigate the influence of overlap. Six different overlaps are considered: 0, 8.3, 16.6, 25, 33 and 42%. In this analysis a rigid roller with radius of  $R = 0.9$  mm is used. The variation of residual stress  $\sigma_{xx}$  along the mention path for five amount of overlap selected is shown in Fig. 7. Furthermore, it shows that increased overlap results in increased magnitude of the maximum residual stress. But 42% overlap causing a surface contraction and cause burr on the surface, so a complete analysis is not possible.



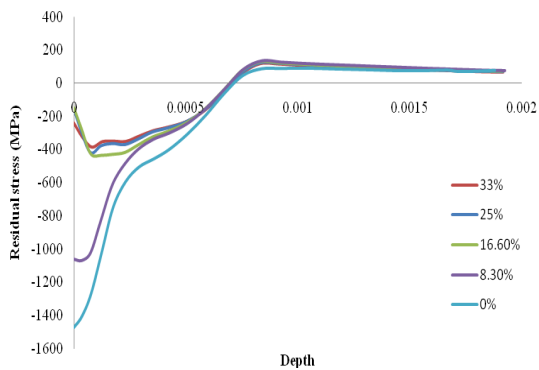


Fig. 7. Variation of overlap

### 5.2 Effect of coefficient friction

The residual stress profile along the mentioned path against the varied coefficient friction is plotted in fig.8. The figure clearly shows that increase in the coefficient of friction results in decrease magnitude of the maximum residual stress and for coefficient of friction  $\mu \geq 0.1$  the effect of friction can cause instability of the diagram. Increased coefficient of friction between the contact workpieces and the roller will cause contraction. To demonstrate this, the Horizontal displacement of a point of the workpiece surface in two cases frictionless and  $f=0.5$  have been compared. This can be observed that moving perpendicular to the surface in the two cases are almost identical. While moving in the direction of rolling in frictionless case is less than other cases.

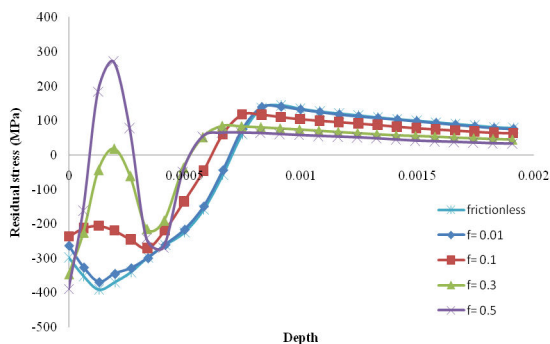


Fig. 8. Effect of coefficient friction

### 5.3 Deep rolling with constant force:

The residual stress profile along the mentioned path against the varied force is plotted in fig.9. As the figure suggests, the increase of rolling force gives rise to the increase of the residual stress up to a specific value of rolling force,  $f=1400$  kN. Further increase in force rolling gives rise to reduction of residual stress. Two substantial cases of diagram can be seen. The first is that the residual stress at a depth more than 0.5 mm for different value of force is almost identical. This indicates that the deep rolling

process is a surface process and changes in the parameters affect only on surface residual stress.

The second is that there is an error in the results at a depth less than 0.1 mm because of the coarse mesh in this area. However due to the high process time a smaller mesh size is not possible. For this reason, the depth, less than 0.1 in conclusion is not considered.

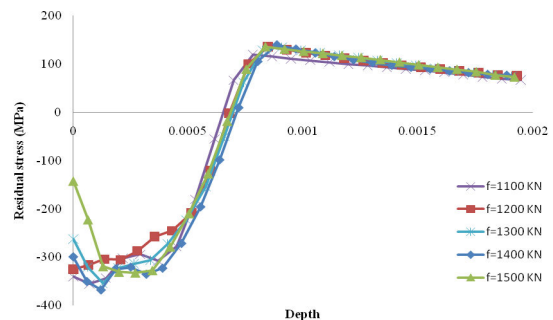


Fig. 9. Deep rolling with constant force on various forces

### 5.4 Deep rolling with mechanical tools

In this case, the pressure required for deep rolling is supplied by the spring force. The processed forces are regulated by changing in the amount of spring compression. Fig.10 shows the variation of residual stress,  $\sigma_{xx}$ , along the mention path for five situation. Fig.10 shows that increase in the spring compression results in largely increase magnitude of the residual stress created in workpiece.

Also, this case compared with a constant force mode as shown in Fig.11. To be able to compare two charts with each other they need to be equal in their forces. In the mechanical method by drawing roller displacement chart versus the processes time we observed that it has a little amplitude. Therefore we can obtain spring force by multiplying initial compression to the spring coefficient. The fig.11 clearly shows the deep rolling with mechanical tools was better than the constant force mode and provides a higher residual stress. And the maximum residual stress in more depth there.

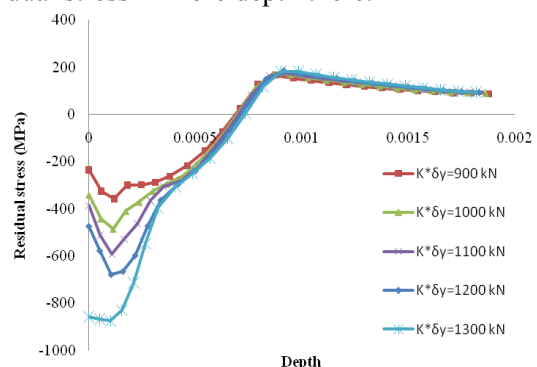


Fig. 10. Deep rolling with mechanical tools

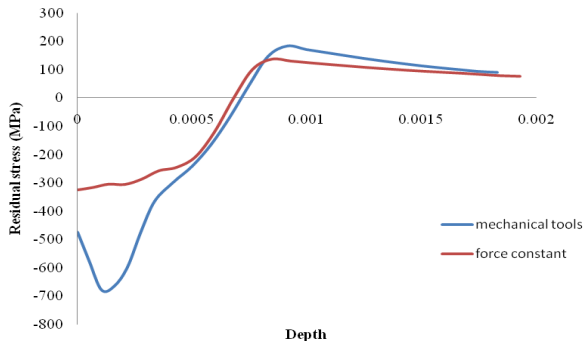


Fig.11. Comparison between two methods of force constant and mechanical tools

### 5.5 Deep rolling with vibration of workpiece

In this section deep rolling is done using the hydrostatic tools and the vibrational with frequency 8 kHz is applied to workpiece. The vibration in xy plane and along the x axis is applied. The result is compared with deep rolling under the same conditions and without vibration. The results are shown in Fig 12.

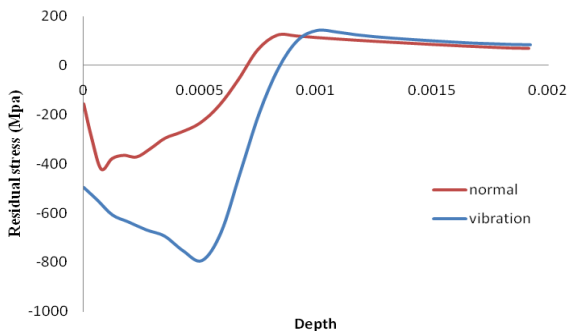


Fig.12. Comparison between deep rolling with vibration and normal method

The figure clearly shows that by using the vibrating workpiece results in largely increase magnitude of the residual stress created in workpiece and increase depth of the compressed residual stress also increase magnitude of the maximum residual stress. This vibration by using constraint displacement and as a periodic is defined and is defined by equation 3.

$$a = A_0 + \sum_{n=1}^N [A_n \cos n\omega(t - t_0) + B_n \sin n\omega(t - t_0)]$$

for  $t \geq t_0$

$$a = A_0 \quad \text{for } t < t_0 \quad (3)$$

Where  $A_0$  is the initial amplitude,  $t_0$  is starting time,  $A$  and  $B$  are amplitude curve and  $\omega$  is Circular frequency. The material constants used in this equation are resented in Table 5.

Table 5: Constants used in equation 3

$A_0$	$A_n$	$B_n$	$N$	$\omega$	$t_0$
0	$10^{-6}$	0	1	52360	0

This is equivalent with the state that the workpiece is stationary and roller has an oscillating velocity. Speed chart in the first step if the workpiece stationary and feed rate oscillating is assumed and normal mode which velocity is constant without fluctuating is shown on Fig 13.

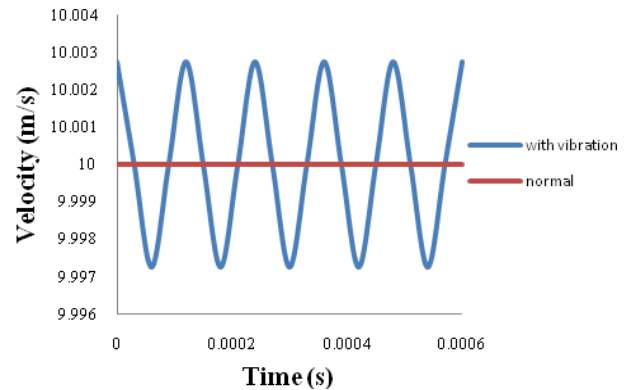


Fig 13: Compare speed in two modes, normal and by using speed fluctuation

## 6 Conclusions

A comprehensive 3D finite element dynamic analysis with considering spring back effect was conducted to simulate the deep rolling process. The model was validated by comparison of the residual stress profiles obtained by simulation and result X-Ray diffraction technique that was proposed by [1]. The effect of overlap of the rolling tracks, friction coefficient between roller and target plate, deep rolling with constant force, deep rolling with mechanical tools, and vibration of workpiece of residual stress  $\sigma_{xx}$  after spring back have been examined and discussed.

The results revealed that increase in overlap of the rolling tracks largely increases the magnitude of the residual stress filed created in target plate. Moreover, increase in the friction coefficient between roller and target plate results in decreases magnitude of the residual stress filed. For high coefficient of friction the effect of friction can cause instability of the diagram. However deep rolling is done in two cases. The first case was constant force. The results revealed that increase in the force intensity results in increase magnitude of the maximum residual stress. Latter was done using mechanical tools. Results showed that increase in the spring compression results in increase

magnitude of the residual stress created in workpiece. Generally all graphs show the fact that for the depth less than 0.1 mm, there is an error in the results because of the coarse mesh in this area. Therefore, this area has been ignored by analyzing. As well as effect of workpiece vibration in the direction of deep rolling was investigated and observed that workpiece vibration results in increase magnitude of the residual stress created in workpiece and increase magnitude of the maximum residual stress.

### References

- [1] Tsuji N, Tanaka S, Takasugi T, "Evaluation of surface-modified Ti-6Al-4V alloy by combination of plasma-carburizing and deep-rolling," *Materials Science and Engineering A* 488 (2008) 139–145
- [2] Mader S, "Festwalzen von Fan- und Verdichterschäufeln," *Dissertation (RWTH Aachen) wt-online* - Ausgabe 6-2008, S. 476-480.
- [3] Klocke F, Bäcker V, Timmer A and Wegner H, "Innovative FE-Analysis of the Roller Burnishing Process for Different Geometries," ed. E Oñate (*Barcelona: CIMNE*) pp 1-4.
- [4] Altenberger I, "Deep Rolling—The Past, the Present and the Future," *Proceedings of 9th International Conference on Shot Peening*, Sept 6–9 (Paris, France), 2005, p 144–155
- [5] Rajesh N, Veeraraghavan S, Ramesh Babu N, "A novel approach for modelling of water jet peening," *J. of Machine Tools & Manufacture*, 44 (2004) 855.
- [6] Altenberger I, Scholtes B, Martin U and Oettel H, "Cyclic deformation and near surface microstructures of shot peened or deep rolled austenitic stainless steel AISI 304," *Materials Science and Engineering A*, 264 (1999) 1.
- [7] Preve'y P.S and Cammett J, "Low Cost Corrosion Damage Mitigation and Improved Fatigue Performance of Low Plasticity Burnished," 7075-T6, *J. Mater. Eng. Perform.*, 2001, 10(5), p 548–555
- [8] Daly J.J, Harrison J.R, and Hackel L.A, "New Laser Technology Makes Laser Shot Peening Commercially Affordable", *Proceedings of 7th International Conference on Shot Peening*, Sept 28–30 (Warsaw, Poland), 1999, p 379–386
- [9] Abramov V.O, Abramov O.V, Sommer F, Gradov O.M, and Smirnov O.M, "Surface Hardening of Metals by Ultrasonically Accelerated Small Metal Balls," *Ultrasonics*, 1998, 36(10), p 1013–1019
- [10] Statnikov E.S, Muktepavel V.O et al., "Efficiency Evaluation of Ultrasonic Impact Treatment (UIT) of Welded Joints in Weldox 420 Steel in Accordance with the IIW Program," *APPLIED ULTRASONICS*, IIW/IIS—DOCUMENT XIII-1817-00, 30 p.
- [11] You-Li Zhu, Kan Wang, Li Li, and Yuan-Lin Huang, "Evaluation of an Ultrasound-Aided Deep Rolling Process for Anti-Fatigue Applications", *Journal of Materials Engineering and Performance*, November 2009, Volume 18(8) , p 1036–1040
- [12] Altenberger I, Stach E.A, Liu G, Nalla R.K, Ritchie R.O, An in situ transmission electron microscope study of the thermal stability of near-surface microstructures induced by deep rolling and laser-shock peening, *Scripta Materialia* 48 (2003) 1593–1598
- [13] Tolga Bozdana A, Nabil N.Z.Gindy, Hua Li, Deep cold rolling with ultrasonic vibrations—a new mechanical surface enhancement technique, *International Journal of Machine Tools & Manufacture* 45 (2005) 713–718
- [14] Juijerm P and Altenberger I, Effect of high-temperature deep rolling on cyclic deformation behavior of solution-heat-treated Al-Mg-Si-Cu alloy, *Scripta Materialia* 56 (2007) 285–288
- [15] Tsuji N, Tanaka S, Takasugi T, Evaluation of surface-modified Ti-6Al-4V alloy by combination of plasma-carburizing and deep-rolling, *Materials Science and Engineering A* 488 (2008) 139–145
- [16] Bäcker V, Klocke F, Wegner H, Timmer A, Grzhibovskis R, Rjasanow S, Analysis of the Deep Rolling Process on Turbine Blades using the FEM/BEM-Coupling, *Materials Science and Engineering* 10 (2010) 012134